Molecular Pharmacology Fast Forward. Published on June 2, 2020 as DOI: 10.1124/mol.120.119719
This article has not been copyedited and formatted. The final version may differ from this version.

Novel c-Myc-targeting Compound, *N*, *N*-Bis (5-ethyl-2-hydroxybenzyl) methylamine, for Mediated c-Myc Ubiquitin–Proteasomal Degradation in Lung Cancer Cells

Nicharat Sriratanasak, Korrakod Petsri, Apirat Laobuthee, Worawat Wattanathana, Chanida Vinayanuwattikun, Sudjit Luanpitpong* and Pithi Chanvorachote*

Department of Pharmacology and Physiology, Faculty of Pharmaceutical Sciences, Chulalongkorn University, Bangkok, Thailand and Cell- based Drug and Health Products Development Research Unit, Faculty of Pharmaceutical Sciences, Chulalongkorn University, Bangkok, Thailand (N.S., K.P., P.C.), Doctor of Philosophy Program in Interdisciplinary Pharmacology, Graduate School,Chulalongkorn University, Bangkok 10330, Thailand (K.P.), Department of Materials Engineering, Faculty of Engineering, Kasetsart University, Ladyao, Chatuchak, Bangkok 10900, Thailand (A.L., W.W.), Division of Medical Oncology, Department of Medicine, Faculty of Medicine, Chulalongkorn University, Pathumwan, Bangkok, Thailand (C.V.), Siriraj Center of Excellence for Stem Cell Research, Faculty of Medicine Siriraj Hospital, Mahidol University, Bangkok, 10700, Thailand (S.L.)

Molecular Pharmacology Fast Forward. Published on June 2, 2020 as DOI: 10.1124/mol.120.119719
This article has not been copyedited and formatted. The final version may differ from this version.

Running title: EMD targets c-Myc for degradation

*Corresponding author:

Pithi Chanvorachote, Ph. D. , Department of Pharmacology and Physiology, Faculty of Pharmaceutical Sciences, and Cell-based Drug and Health Product Development Research Unit, Chulalongkorn University, Bangkok, Thailand

Tel: (662) 218-8285, Fax: (662) 218-8340

Email: pithi.ch@gmail.com

Sudjit Luanpitpong, Ph.D., Siriraj Center of Excellence for Stem Cell Research, Faculty of Medicine Siriraj Hospital, Mahidol University, 2 Siriraj Hospital, Bangkoknoi, Bangkok, Thailand

Tel.: (662) 419-2907

Email: suidjit@gmail.com

The number of text pages: 41

The number of tables: 1

The number of references: 69

The number of words in the *Abstract*: 195

The number of words in the *Introduction*: 639

The number of words in the *Discussion*: 1322

Molecular Pharmacology Fast Forward. Published on June 2, 2020 as DOI: 10.1124/mol.120.119719
This article has not been copyedited and formatted. The final version may differ from this version.

Abbreviations

AKT, protein kinase B; BSA, bovine serum albumin; CHX, cycloheximide; DMEM, Dulbecco's Modified Eagle Medium; DMSO, dimethyl sulfoxide; EDTA, Ethylenediaminetetraacetic acid; EMD, *N*, *N*-bis (5-ethyl-2-hydroxybenzyl) methylamine; FBS, fetal bovine serum; IMDM, Iscove's Modified Dulbecco's Medium, MTT, 3- (4,5- dimethylthiazol- 2- yl) - 2,5- diphenyltetrazolium bromide; NSCLC, non- small- cell lung carcinoma; PBS, phosphate buffer saline; PI, propidium iodide; RPMI, Roswell Park Memorial Institute; Uq, ubiquitin

Molecular Pharmacology Fast Forward. Published on June 2, 2020 as DOI: 10.1124/mol.120.119719
This article has not been copyedited and formatted. The final version may differ from this version.

Abstract

Aberrant c-Myc is a common feature in the majority of human cancers and has been linked to oncogenic malignancies. Here, we developed a novel c-Myc-targeting compound, *N*, *N*-bis (5-ethyl-2-hydroxybenzyl) methylamine (EMD), and present evidence demonstrating its effectiveness in targeting c-Myc for degradation in human lung carcinoma. EMD exhibited strong cytotoxicity toward various human lung cancer cell lines ae well as chemotherapeutic-resistant patient-derived lung cancer cells through apoptosis induction, in comparison to chemotherapeutic drugs. The half-maximal inhibitory concentration (IC_{50}) of EMD against lung cancer cells was approximately 60 μM. Mechanistically, EMD eliminated c-Myc in the cells and initiated caspase-dependent apoptosis cascade. Cycloheximide chase assay revealed that EMD tendentiously shortened the half-life of c-Myc by approximately half. The cotreatment of EMD with the proteasome inhibitor MG132 reversed its c-Myc-targeting effect, suggesting the involvement of ubiquitin-mediated proteasomal degradation in the process. We further verified that EMD strongly induced the ubiquitination of c-Myc and promoted protein degradation. c-Myc inhibition and apoptosis induction were additionally shown in hematologic malignant K562 cells, indicating the generality of the observed EMD effects. Altogether, we identified EMD as a novel potent compound targeting oncogenic c-Myc, which may offer new opportunities for lung cancer treatment.

Keywords c-Myc; apoptosis, lung cancer, targeted therapy, protein degradation, EMD

Molecular Pharmacology Fast Forward. Published on June 2, 2020 as DOI: 10.1124/mol.120.119719
This article has not been copyedited and formatted. The final version may differ from this version.

Significance Statement

The deregulation of c-Myc is frequently associated with cancer progression. This study examined the effect of a new compound, namely *N*, *N*-bis (5-ethyl-2-hydroxybenzyl) methylamine (EMD), in targeting c-Myc in several lung cancer cell lines and drug-resistant primary lung cancer cells. EMD induced dramatic c-Myc degradation through a ubiquitin–proteasomal mechanism. The promising anticancer and c-Myc-targeted activities of EMD support its use in potential new approaches to treat c-Myc-driven cancer.

Introduction

For many decades, lung cancer has ranked among the top causes of cancer related-deaths (Siegel *et al.*, 2016; Siegel *et al.*, 2019). Non-small cell lung cancer (NSCLC) is the predominant type that can be found in more than 80% of all lung cancer patients. The five-year survival rate of NSCLC is less than 20% and most patients tend to be diagnosed at an advanced metastasis stage (Siegel *et al.*, 2019; Goebel *et al.,* 2019). The poor prognosis of NSCLC patients depends a lot on their level of resistance to conventional cancer treatment, such as surgery, chemotherapy, and radiation (Zappa and Mousa, 2016; Vansteenkiste *et al.*, 2013; Reck *et al.*, 2014). Hence, finding a novel rational approach to improve the NSCLC response to therapy is a most interesting proposition. Targeting oncogenes and/or key regulatory proteins that control oncogenic processes and cancer aggressiveness is a promising approach for novel cancer therapy (Baig *et al.*, 2016).

The proto-oncogene *MYC,* encoded for a c-Myc protein, functions as a transcription factor and key effector in cellular signaling, which plays enormous roles in controlling biological functions and cellular processes (Pelengaris *et al.*, 2002). The aberrant expression of c-Myc has been observed in a broad range of human cancers (Kalkat *et al.*, 2017; Daniell, 2012) and has been linked to almost every aspect of the oncogenic process, including orchestrating uncontrolled tumor growth and proliferation, immortalization, escape from immune surveillance, and rendering treatment-resistance (Zahavi and Weiner, 2019; Carabet *et al.*, 2019). c-Myc is crucial for the pathogenesis of lung cancer (Dragoj *et al.*, 2019; Stine *et al.*, 2015), and has been found to be overexpressed and highly activated by means of biological activity (Kalkat *et al.*, 2017). Previous studies showed that c-Myc inhibition resulted in the restoration of checkpoint mechanisms, growth arrest, and senescence as well as a greater

responsiveness to chemotherapy (Gabay *et al.*, 2014; Felsher and Bishop, 1999; Zhang *et al.*, 2017; Allen-Petersen *et al.*, 2019; Bressin *et al.*, 2006).

A considerable number of studies and reviews have highlighted the importance of new approaches to treat Myc-driven cancers by directly managing the c-Myc protein or its downstream effectors (Vita and Henriksson, 2006; Carabet *et al.*, 2019; Chen *et al.*, 2018; Huang *et al.*, 2014; Whitfield *et al.*, 2017). A number of strategies to target c-Myc for cancer therapeutic purposes have been exploited. The stability of c-Myc relies on two phosphorylation sites at serine 62 (S62) and threonine 58 (T58), which are controlled by the function of extracellular signal-regulated kinase (ERK) and glycogen synthase kinase-3β (GSK-3β), respectively. While phosphorylation at S62 causes the protein to become more stable, phosphorylation at T58 facilitates the ubiquitin–proteasomal degradation (Farrell and Sears, 2014; Conacci-Sorrell *et al.*, 2014; Amati and Sanchez-Arévalo Lobo, 2007). The T58 phosphorylation induces the recognition and ubiquitination of c-Myc by the E3 ligase FBW7. c-Myc is polyubiquitinated by FBW7 and subsequently degraded by the proteasome. As the degradation of c-Myc through the proteasomal mechanism generally dominates in the cells, the c-Myc protein has a relatively short half-life (approximately 20–30 minutes) (Farrell and Sears, 2014; Amati and Sanchez-Arévalo Lobo, 2007).

EMD is a newly synthesized compound that was fabricated by a two-step Mannich reaction and ring-opening dimerization using 4-ethylphenol, formaldehyde, and methylamine in the ratio of 1:2:1 as precursors. After this, colorless single crystals were obtained. The characteristics of EMD were evaluated by Fourier transform infrared spectroscopy (FTIR) and proton nuclear magnetic resonance spectroscopy (^{1}H-NMR) (Chirachanchai *et al.*, 2009; Veranitisagul *et al.*, 2011; Wattanathana *et al.*, 2016). The identified chemical derivative structures have previously been shown to trigger apoptotic cell death in various cancer cell types (Kumar *et al.*, 2019), yet their function to target c-Myc has never been explored.

Molecular Pharmacology Fast Forward. Published on June 2, 2020 as DOI: 10.1124/mol.120.119719
This article has not been copyedited and formatted. The final version may differ from this version.

Consequently, this research was an exploratory study aimed at investigating the potential clinical utility of EMD by testing its roles in apoptosis induction and c-Myc inhibition.

Molecular Pharmacology Fast Forward. Published on June 2, 2020 as DOI: 10.1124/mol.120.119719
This article has not been copyedited and formatted. The final version may differ from this version.

Materials and Methods

Synthesis of EMD

Paraformaldehyde ($(CH_2O)_n$) was purchased from Sigma (U.S.A.). The chemicals, 4-ethylphenol (p-$C_2H_5C_6H_4$-OH, methylamine (CH_3NH_2) (40% w/v in water), and propan-2-ol were purchased from Fluka Chemicals. Sodium hydroxide (NaOH) and anhydrous sodium sulfate (Na_2SO_4) were obtained from Ajax Finechem and Merck, respectively. Dichloromethane (CH_2Cl_2), diethyl ether ($CH_3CH_2OCH_2CH_3$), and dioxane solvents were received from RCI Labscan. All chemicals were analytical grade and used as received.

The benzoxazine dimer, EMD was synthesized according to the reaction scheme illustrated in Figure 1A (Chirachanchai *et al.*, 2009; Veranitisagul *et al.*, 2011; Wattanathana *et al.*, 2016). Two consecutive steps, namely Mannich reaction (Step 1) and ring-opening dimerization (Step 2), needed to be carried out. For the first step, three starting materials, 4-ethylphenol, formaldehyde, and methylamine, were mixed in a round bottom flask with the molar ratio of 1:2:1 (Kaewvilai *et al.*, 2012; Wattanathana *et al.*, 2014). The mixture was then refluxed for 6 h in dioxane solvent until the reaction went to completion resulting in the clear yellow solution. The obtained solution was washed with 3N NaOH solution and distilled water to remove impurities. The dioxane solvent was removed later using a rotary evaporator so that the pure compound of 6-ethyl-3-methyl-3,4-dihydro-*2H*-benzo[e][1,3]oxazine (EM) was obtained in the form of sticky brown liquid. For the second step, the equimolar amount of 4-ethylphenol was added to the obtained compound EM without any other solvent and then heated at 60 °C for 8 h to get the EMD compound. The crude product of the compound EMD was washed with diethyl ether to remove impurities and to get the white precipitate of the compound EMD. Further purification of the EMD compound was carried out by recrystallization of the white precipitate of the compound EMD. The colorless single crystals were obtained after left the

alcoholic solution for several days. The purity of the EMD compound was more than 99%. The crude product from synthesis was washed three times using diethyl ether. Moreover, further purification was done by crystallization. The obtained crystals exhibited a very sharp melting point, and no impurity peaks were observed in the 1H-NMR spectrum.

Reagents and antibodies

RPMI 1640 medium, DMEM, IMDM, FBS, penicillin/streptomycin, L-glutamine, PBS, and trypsin-EDTA were obtained from Gibco (Grand Island, NY, USA). MTT, DMSO, Hoechst 33342, CHX, MG132, and BSA were purchased from Sigma-Aldrich, Co. (St. Louis, MO, USA). The primary antibodies, c-Myc (#5605), Poly (ADP-ribose) polymerase or PARP (#9532), caspase-3 (#9662), caspase-9 (#9502), Bcl-2 (#4223), Akt (#9272), phosphorylated Akt or p-Akt (#4060), and β-actin (#4970) were acquired from Cell Signaling Techbology (Danvers, MA, USA). The primary antibody ubiquitin (ab7780) was obtained from Abcam (Cambridge, UK). The secondary antibody, anti-rabbit IgG (#7074) were obtained from Cell Signaling Technology (Danvers, MA, USA). The tested compound, EMD was synthesized by the procedure shown in following section.

Preparation of EMD stock solution

EMD was prepared as a 40 mM master stock solution by dissolving in DMSO and then diluted to 2 mM, 4 mM, 6 mM, 10 mM, 15 mM and 20 mM stock solutions. All of the stock solutions were stored at -20°C and were freshly diluted 200 times with RPMI, IMDM or DMEM completed medium to the required concentrations before treatment. The final concentrations of DMSO in all treatment conditions were less than 0.5% v/v.

Molecular Pharmacology Fast Forward. Published on June 2, 2020 as DOI: 10.1124/mol.120.119719
This article has not been copyedited and formatted. The final version may differ from this version.

Cell lines and culture

Human NSCLC-derived H23 (ATCC®CRL 5800™) and H292 (ATCC ®CRL 1848™) cells were cultured in 10% FBS RPMI with 1% penicillin and streptomycin, while human chronic myeloid leukemia-derived K562 (ATCC ®CRL 243™) cells were cultured in 10% FBS IMDM with 1% penicillin and streptomycin. Human keratinocyte HaCAT cells (Cell Lines Service Heidelberg, Germany) and human kidney HK2 cells (ATCC ® CRL-2190™) were cultured in 10% FBS DMEM with 1% penicillin and streptomycin. The cells were maintained at 37°C in a humidified incubator of 5% carbon dioxide. About 85% confluence of cells were applied for dosing experiments in this study.

Protocol for primary lung cancer cell establishment.

The patient-derived primary lung cancer cells were obtained from pleural effusion (500-1000 ml) by thoracentesis and collected aseptically in heparinized. Samples were centrifuged at 300 g for 10 min, at 4°C, and cell pellet was resuspended in 10% FCS-RPMI (Invitrogen, MA, USA). Viability was first determined by the Trypan Blue exclusion dye. After a harvesting and 2 rounds of washing, the cells were subjected to the cell cultivation for about 10-15 passages. The study and protocol were approved by the Ethics Committee of the Faculty of Medicine, Chulalongkorn University, Bangkok, Thailand (IRB 365/62) and complied with declaration of Helsinki. Written informed consent was obtained from all the participants.

Cytotoxicity assay

For cytotoxicity assay, 1.5 x 10^4 cells/well of lung cancer cells were seeded onto 96-well plates and incubated overnight. After that cells were treated with various concentrations of EMD for 24 hours at 37°C and analyze by using MTT assay according to manufacturer's protocol (Sigma Chemical, St. Louis, MO, USA). In calculating the cell viability, measured

absorbance of treated cells will be divided by the value of non-treated cells and report in percentage.

Nuclear staining assay

This method was applied to define apoptotic and necrotic cell death by using nuclear staining with Hoechst 33342. The cells were seeded on 96-well plates at the density of 1.5 × 10^4 cells/well and provided to incubate overnight. The cells were treated with various concentrations of EMD and incubated for 24 hours at 37°C. Afterwards, the cells were incubated with 10 µg/ml of Hoechst 33342 for 30 minutes at 37°C. Then, they were visualized and imaged under a fluorescence microscope (Nikon ECLIPSE Ts2). Results had been reported in percentage of apoptotic cells.

Annexin V-FITC/PI flow cytometry

This method was introduced to examine apoptotic cell death by using flow cytometry with Annexin V-FITC/PI staining. H292 and H23 were seeded on 24-well plates at concentration of 1 x 10^5 cells/well and incubated overnight. The cells were treated with various concentrations of EMD and incubated for 24 hours at 37°C. At the end of incubation time, they were detached from the well surface by using trypsin-EDTA (0.25%). The cells were incubated with 5 µL of Annexin V-FITC and 1 µL of PI for 15 minutes at room temperature in dark. After that, the cells had been analyzed by guavaCyte™ flow cytometry systems (guavasoft™ Software version 3.3).

Molecular Pharmacology Fast Forward. Published on June 2, 2020 as DOI: 10.1124/mol.120.119719
This article has not been copyedited and formatted. The final version may differ from this version.

Cell cycle analysis

Cell cycle progression was evaluated by using flow cytometry with Hoechst 33342 staining. H292 and H23 cells were seeded onto 6-well plates at concentrations of 5 x 10^5 cells/well. After that the cells were treated with various concentration of EMD for 24 hours. At the end of incubation time, they were detached from the well surface by using trypsin-EDTA (0.25%). Non-treated cells and boiled cells represented live cells and death cells respectively. The cells were incubated with 5 µg/ml Hoechst 33342 for 30 minutes at 37°C. Then, the cells had been analyzed by BD FACSDiva 8.0.2 flow cytometry systems.

Western blot analysis

The cells were seeded on 6-well plates at the density of 5 x 10^5 cells/well and incubated overnight. After EMD treatment, the apoptosis cells were collected by centrifuging media with 1500 rpm for 5 minutes and aspirated supernatants. The cells were incubated with RIPA lysis buffer containing 25 mM Tris-HCl pH 7.6, 150 mM NaCl, 1% NP-40, 1% sodium deoxycholate, 0.1% SDS for 30 minutes at 4°C. The lysates were collected, and their protein contents were determined using a BCA protein assay kit (Pierce Biotechnology, Rockford, IL, USA). Equivalent amount of proteins from each sample was separated by SDS-PAGE and transferred to 0.2 µm polyvinylidene difluoride (PVDF) membranes (Bio-Rad). The separating blots were blocked with 5% skim milk in TBST (Tris-buffer saline with 0.1% tween containing 25 mM Tris-HCl pH 7.5, 125 mM NaCl and 0.1% tween 20) for 2 hours and incubated with primary antibody against caspase-3, caspase-9, PARP, Akt, p-Akt, Bcl-2, c-Myc and beta-actin overnight at 4°C. Then, the membranes were incubated with secondary antibody for 2 hours at room temperature after washed by TBST three times. Finally, the protein bands were detected using chemiluminescence substrate and exposed by Chemiluminescent ImageQuant LAS4000.

Molecular Pharmacology Fast Forward. Published on June 2, 2020 as DOI: 10.1124/mol.120.119719
This article has not been copyedited and formatted. The final version may differ from this version.

Protein band had been analyzed using Image J software (version 1.52, National Institutes of Health, Bethesda, MD, USA).

Protein stability by cycloheximide (CHX) chase assay

The cells were seeded on 6-well plates at the density of 5 x 10^5 cells/well and incubated overnight. Then, the cells were treated with CHX with or without 100 μM of EMD for 0,15,30,45 and 60 minutes. The treated cells were collected and lysed with RIPA lysis buffer. Western blot analysis was performed for evaluating c-Myc protein levels. Protein bands had been analyzed using Image J software (version 1.52, National Institutes of Health, Bethesda, MD, USA) and protein half-life was calculated.

Ubiquitin-dependent protein degradation

5 x 10^5 cells/well of lung cancer cells were seeded on 6-well plates and left for attachment overnight. Then, cells were treated with 100 μM of EMD after pretreatment with various concentrations of MG132 (0-20 μM). Non-treated cells were used as a control. All of the cells were collected and lysed with RIPA buffer. Western blot analysis was performed for evaluating C-myc protein levels. Protein band had been analyzed using Image J software (version 1.52, National Institutes of Health, Bethesda, MD, USA).

Immunoprecipitation assay

H292 and H23 lung cancer cell lines were pre-treated with MG132 10 μM for 30 minutes followed by EMD 100 μM for 1 hour. The treated cells were collected and lysed with RIPA buffer. The magnetic beads from Dynabeads™ Protein G Immunoprecipitation Kit from Thermo Fisher Scientific Inc. (Waltham, MA, USA) were irrigated with washing buffer and

Molecular Pharmacology Fast Forward. Published on June 2, 2020 as DOI: 10.1124/mol.120.119719
This article has not been copyedited and formatted. The final version may differ from this version.

incubated with primary antibody (Ab) of c-Myc in binding buffer for 10 minutes. Protein lysate was mixed with bead-Ab complex at 4°C overnight. Then, the bead-Ab-antigen (Ag) complex was washed three time with 200 μL washing buffer. Supernatant was removed and elution buffer was added for detaching the Ab-Ag complex from the beads. After that, western blot analysis was performed to detect the ubiquitinated c-Myc protein.

Statistical analysis

The results were presented in mean ± SD of at least 3 independent determinations performed in triplicate. Each sample containing at least $1.5x10^4$ cells was analyzed. Multiple comparisons for statistically significant differences between multiple groups (ANOVA) was calculated using SPSS software program version 16 (SPSS Inc., Chicago, IL, USA), followed by individual comparisons with Schefft's post-hoc test. For two-group comparisons, t-test was calculated by SPSS software program. Statistical significance was considered at $p < 0.05$. GraphPad prism 5 was used for creating graphs in all experiments. Calculated *p*-value cannot be interpreted as hypothesis-testing but only as descriptive.

Molecular Pharmacology Fast Forward. Published on June 2, 2020 as DOI: 10.1124/mol.120.119719
This article has not been copyedited and formatted. The final version may differ from this version.

Results

Characterization of EMD

Pure crystals of the EMD compound were characterized by Fourier transform infrared spectroscopy (FTIR) and proton nuclear magnetic resonance spectroscopy (^{1}H-NMR) to confirm the structural identity. For the FTIR study, crystals of the pure EMD compound were ground with potassium bromide (KBr) and then uniaxially pressed into a pellet prior to measurement. Then, 100 FTIR scans were performed in the range of 4000–375 cm^{-1} with a spectral resolution of ±2 cm^{-1} using a Bruker Alpha FTIR spectrometer. The ^{1}H-NMR investigation was performed on a Varian Mercury-400 spectrometer. A few milligrams of the pure compound were dissolved in $CDCl_3$ before the ^{1}H-NMR measurements.

Both the FTIR and 1H-NMR results confirmed the successful synthesis of the EMD compound as identified by the presence of the characteristic vibrational and resonance peaks as follows: **FTIR** (KBr, cm^{-1}): 3281 (br, OH), 1498 (vs, C-C in oxazine ring), 1456 (m, N-CH_3), 1274 (s, C-N), 1205 (m, C-N-C), 821 (vs, C-N-C) (Figure 1B).

^{1}H-NMR (400 MHz, $CDCl_3$, ppm): δH 1.25 (t, 6H, R-C**H**$_3$), 2.30 (s, 3H, N-C**H**$_3$) 2.60 (q, 4H, Ar-C**H**$_2$-CH_3), 3.66 (s, 4H, Ar-C**H**$_2$-N), 6.78 (d, 2H, Ar-**H**), 6.93 (d, 2H, Ar-**H**), 6.99 (s, 2H, Ar-**H**). Our group also reported the crystal structure of the EMD compound at 298 K in the supporting material of our previous work (Figure 1C), which support the present results from the FTIR and 1H-NMR analyses.

EMD induces apoptosis in human lung carcinoma cells

To investigate the potential anticancer activity of EMD in human lung carcinoma, its cytotoxicity was first evaluated. NSCLC H23 and H292 cells were treated with various concentrations of EMD (0–100 μM) for 24 hours and then cell viability was analyzed by MTT

Molecular Pharmacology Fast Forward. Published on June 2, 2020 as DOI: 10.1124/mol.120.119719
This article has not been copyedited and formatted. The final version may differ from this version.

assay. All of the data was calculated based on results of 3 replicated samples. The results showed that EMD significantly reduced cell viability in H23 and H292 cells in a concentration-dependent manner when compared with non-treatment controls (Figure 2A). The IC_{50} values of EMD in both cell lines are presented in Figure 2B. The values were calculated from single values based on equations fitted to the pooled data. A nuclear staining assay was further performed to evaluate the mode of cell death induced by EMD. Morphological changes by means of condensed and/or fragmented nuclei were observed after the treatment for 24 hours, indicating that both cell lines encountered apoptotic cell death significantly after treatment with 75 μM of EMD when compared with the non-treatment control (Figures 2C–D).

Flow cytometry analysis using annexin V-FITC/PI was applied to validate the apoptotic cell death induced by EMD. Similar to the nuclear staining assay, EMD significantly induced apoptotic cell death, starting at a concentration of 75 μM in H23 cells, but at 100 μM in H292 cells (Figures 2E–F). To further confirm the EMD apoptotic activity, cell cycle analysis was performed using flow cytometry and Hoechst 33342 staining as a DNA dye. The result showed that after EMD treatment at various concentrations (0–100 μM) for 24 hours, the sub G1 phase, representing DNA fragmentation in apoptotic cells, was increased in a concentration-dependent manner in both H292 and H23 cells (Figures 2G–H), thus confirming apoptosis as the mechanism of the EMD-induced cytotoxicity.

EMD triggers apoptosis cascade through mechanisms that involve c-Myc downregulation

The activation of caspases and the cleavage of their cellular substrate PARP are known to initiate an apoptosis cascade, making them well-known apoptotic markers. NSCLC H292 and H23 cells were treated with EMD (0–100 μM) for 24 hours, after which the total cells were collected and PARP, caspase-3, caspase-9, and their cleaved forms were evaluated by western blot analysis. Same as previous experiments, all of the data was calculated based on results of

Molecular Pharmacology Fast Forward. Published on June 2, 2020 as DOI: 10.1124/mol.120.119719
This article has not been copyedited and formatted. The final version may differ from this version.

3 replicated samples. Figures 3A and B show that EMD significantly cleaved and activated caspase-3 and caspase-9, while it caused PARP cleavage and inactivation when compared to the non-treated control (Figures 3A–B).

The drug sensitivity of tumor cells in response to certain treatments, including conventional chemotherapy, is tightly regulated by the interactions between pro-survival and apoptotic signals, which act to tweak the balance between survival and cell death. To elucidate the underlying mechanisms of apoptosis induction by EMD, we monitored the expression levels of the key pro-survival proteins, i.e., Akt and phosphorylated Akt (p-Akt), and anti-apoptotic Bcl-2 protein in EMD-treated H292 and H23 cells. We found that the ratio of p-Akt/Akt and Bcl-2 levels were not notably changed after EMD treatment at the concentrations that induced apoptosis, leading us to the discovery of other targets that are important in NSCLC drug response and that may be associated with EMD.

c-Myc is an essential protein for tumor cell maintenance and is a central oncogenic switch. In lung cancer, the inactivation of c-Myc can induce apoptotic cell death and lead to cancer regression and induce apoptotic cell death (Daniel *et al.,* 2012; Pelengaris *et al.,* 2002). We tested the effect of EMD treatment on c-Myc and found a dramatic downregulation of c-Myc in response to EMD at 24 hours, even at the lowest concentration of 50 μM. At higher concentrations of EMD, i.e., 100 μM, the level of c-Myc had almost disappeared in all the tested cells (Figures 3C–D). These results indicate that c-Myc is a preferable molecular target of EMD and that the possible mechanism of action of EMD may be related to c-Myc degradation.

EMD shortens c-Myc half-life through the induction of c-Myc proteasome degradation

One of the strategies for targeting c-Myc for cancer treatment is the promotion of c-Myc degradation (Vita and Henriksson, 2006). Having demonstrated the dramatic c-Myc downregulation by EMD, we further identified its mechanism of c-Myc regulation. A protein abundance reflects the balance of the rates of protein synthesis and protein degradation. To substantiate whether EMD affected c-Myc degradation, we used the protein biosynthesis inhibitor CHX to prevent translational elongation (Kao *et al.*, 2015) and performed a CHX chase assay to estimate the half-life of c-Myc in NSCLC H292 and H23 cells. Here, the cells were treated with 50 μg/ml of CHX with or without 100 μM EMD and western blot analysis was performed at various time (0–60 minutes) to determine the c-Myc level (Figures 4A–B). We observed that c-Myc started to degrade significantly at 15 minutes in the non-treated cells and that EMD treatment in both H292 and H23 cells induced c-Myc degradation. The half-lives of c-Myc in the non-treated control and EMD-treated cells were calculated and the results are shown in Figure 4C. The values were calculated from single values based on equations fitted to the pooled data. The results demonstrated that c-Myc degraded much faster and its stability was reduced in EMD-treated cells when compared to the non-treated cells.

Ubiquitin–proteasome degradation has been shown to influence protein turnover. Thus, MG132, a potent proteasome inhibitor, was applied to verify that c-Myc destability by EMD occurred in this degradation mechanism. After EMD treatment in H292 and H23 cells, the c-Myc protein level decreased within 1 hour (Figures 4D–E). Remarkably, the addition of MG132 (0–20 μM) to EMD treatment restored the c-Myc protein level, indicating that c-Myc degradation occurred through the ubiquitin–proteasome system. We also checked the premise of ubiquitin-mediated c-Myc degradation using co-immunoprecipitation and evaluated the level of the c-Myc-ubiquitin complex (poly Ub-c-Myc) in H292 and H23 cells after treatment with 100 μM of EMD and in non-treated control cells for 1 hour. Figures 4F–G show that the

Molecular Pharmacology Fast Forward. Published on June 2, 2020 as DOI: 10.1124/mol.120.119719
This article has not been copyedited and formatted. The final version may differ from this version.

polyubiquitination of c-Myc was noticeably elevated after EMD treatment when compared with the non-treated control, thus confirming that EMD mediated c-Myc stability through ubiquitin–proteasome degradation.

EMD could decrease the c-Myc protein level in other cancerous primary lung cancer and normal cells

This section outlines how EMD not only had a universal effect on lung cancer cell lines but also affected other cancerous cells. Hence, K562 CML cells and four primary cell lines, namely ELC12, ELC16, ELC17, and ELC20, derived from adenocarcinoma lung cancer patients were used for evaluating the anticancer property of EMD. ELC12, ELC16, and ELC 17 cells were collected from patients who had not received any chemotherapy, while ELC20 cells were collected from a patient who had already received chemotherapy (Vinayanuwattikun *et al.*, 2019). The characterization of each primary cell line is presented in Table 1.

The morphology change of K562 cells was observed under a fluorescence microscope after Hoechst 33342 staining. The results indicated that apoptotic cell death was significantly induced in a concentration-dependent manner after 0–100 μM EMD treatment for 24 hours (Figures 5A–B). Then, the c-Myc protein levels were evaluated by western blot analysis after treatment with EMD (0–100 μM) for 24 hours. Surprisingly, the protein levels were decreased, similar to the results in lung cancer cell lines, when compared with non-treated cells (Figures 5C–D).

MTT assay and nuclear staining assay were used for evaluating the cell viability and apoptotic cell death of the four primary lung cancer cell lines, respectively. We used the chemotherapeutic drug etoposide for comparison. After treatment with various concentrations of EMD (0–100 μM) or etoposide at the same concentrations, the results showed that EMD

had superior apoptotic-inducing activity than etoposide at the concentration of 75 μM in the first three cell lines and at 100 μM in ELC20. EMD significantly decreased cell viability and mediated apoptotic cell death in all four primary cancer cells (Figures 5E–I). The half-maximal inhibitory concentrations (IC_{50}) of EMD on the four primary cell lines were calculated. The values were calculated from single values based on equations fitted to the pooled data. As etoposide is a standard drug used for treatment of lung cancer (Ruckdeschel, 1991; Comis et al., 1999; Cosaert and Quoix, 2002) and evidences indicated that etoposide is effective in treatment of lung cancer when used alone or in combination with other chemotherapeutic drugs (Furuse, 1992; Sallam et al., 2019), the observed resistance of primary lung cancer cells in this experiment was unexpected and the resistance may cause by specific properties of certain cells.

Moreover, western blot analysis was performed to evaluate the c-Myc protein levels after 100 μM of EMD treatment in all four primary cell lines. The results showed that the c-Myc protein levels in all four primary cell lines were significantly decreased compared with those of the non-treatment control (Figures 5J–K). We thus confirmed the effect of EMD in mediating c-Myc degradation by MG132 treatment in K562 and primary lung cancer cells. The results demonstrated that the addition of MG132 could restore the effect of EMD in downregulating the c-Myc protein (Figures 5L–M).

We also determined the effect of EMD on c-Myc in non-cancerous human keratinocyte HaCAT and renal epithelial HK2 cells. The results revealed that treatment of the cells with EMD caused a dramatic reduction of the c-Myc protein in HaCAT cells, while EMD only slightly decreased the c-Myc protein level in HK2 cells (Figures 5N–O). These results indicate that EMD is a new capable candidate compound for the treatment of lung cancer. Indeed, EMD demonstrated a potential to decrease cell viability and increase apoptotic cell death in cells derived from lung cancer patients. These results further suggest that EMD may be a new candidate compound for cancer treatment in patients resists to existing chemotherapy.

Molecular Pharmacology Fast Forward. Published on June 2, 2020 as DOI: 10.1124/mol.120.119719
This article has not been copyedited and formatted. The final version may differ from this version.

Discussion

As is well known, cancer cells have a fallibility in terms of the apoptotic pathway. These defects not only promote cancer progression, but can also render therapeutic failure (Igney and Krammer, 2002). One way to perform cancer treatment is through activation of the death mechanism within cancer cells, where targeting the apoptosis pathway is the most successful. The apoptosis mechanism can be evaluated by tracking the pro-apoptotic or anti-apoptotic markers and caspase enzyme cascade (Pollard *et al.*, 2017; Bock and Tait, 2019). c-Myc is an oncoprotein that has been shown to be important for the proliferation and progression of lung cancer (Allen-Petersen and Sears, 2019), including therapeutic resistance and a poor prognosis (Pan *et al.*, 2014; Knapp *et al.*, 2003; Xia *et al.*, 2015; Elbadawy *et al.*, 2019). Much research data have indicated that most cancers develop mechanisms to elevate c-Myc activities to promote cell survival, proliferation, and invasiveness (Daniell, 2012). A series of reports exhibited that c-Myc inhibition may lead to tumor regression. In this study, we found that treatment with EMD resulted in a significant induction of the caspase cascade but had minor effects on other apoptotic markers (Figure 3). In contrast, our protein of interest, i.e., c-Myc, was strongly affected by EMD treatment (Figures 3C–D).

EMD is a benzoxazine dimer synthesized from 4-ethylphenol, formaldehyde, and methylamine in two steps, comprising a Mannich reaction and ring-opening dimerization (Chirachanchai *et al.*, 2009; Veranitisagul *et al.*, 2011). As this is a newly synthesized compound, data on this compound are limited, although a previous study showed that benzoxazine derivatives could induce apoptosis in various cancerous cell types, such as breast cancer, cervical cancer, and osteosarcoma (Kumar *et al.*, 2019).

Emerging evidence favors the use of c-Myc-targeted therapy for cancer treatment (Huang *et al.*, 2014; Whitfield *et al.*, 2017; Brägelmann *et al.*, 2017). A previous study revealed that

Molecular Pharmacology Fast Forward. Published on June 2, 2020 as DOI: 10.1124/mol.120.119719
This article has not been copyedited and formatted. The final version may differ from this version.

the increased stability of c-Myc plays a role in the pathogenesis of certain cancers (Gregory and Hann, 2000). As the level of the c-Myc protein is shown to be regulated through ubiquitin–proteasome protein degradation (Sears, 2004), targeting c-Myc by facilitating the protein degradation may offer a strategy for drug action in c-Myc-driven cancers. So far, several small molecules have been shown to be able to effectively promote c-Myc degradation, such as oridonin (Huang *et al.,* 2012) and MLN8237 (Li *et al.,* 2018). Oridonin is a natural compound that suppresses tumor cell growth and induces apoptosis by driving the Fbw7-mediated ubiquitin–proteasomal degradation of c-Myc (Huang *et al.,* 2012). Likewise, MLN8237, an aurora A kinase inhibitor, was shown to dramatically induce c-Myc degradation via a proteasomal pathway in thyroid cancer and to contribute to anticancer activity *in vitro* and in xenograft tumor models (Li *et al.,* 2018).

Another approach focused on the stabilization of c-Myc. It is known that the c-Myc protein is stabilized by phosphorylation at serine 62 of the c-Myc protein (Sears *et al*., 2000). While the tumor suppressor protein phosphatase 2A (PP2A) dephosphorylates such a serine phosphorylation and destabilizes c-Myc, the endogenous inhibitors of PP2A, which are SET oncoprotein and the cancerous inhibitor of PP2A (CIP2A), have been found to be overexpressed in certain cancers, and the function of these, i.e., SET and CIP2A, resulted in c-Myc stabilization (Westermarck *et al.,* 2008; Come *et al*., 2009). In addition, a study indicated that the augmented expression of CIP2A is linked with poor prognosis and the aggressiveness of lung cancer (Cha *et al.,* 2017). The SET antagonist OP449 was shown to suppress the tumorigenic potential of cancer cells, induce apoptosis cell death, and enhance the effects of tyrosine kinase inhibitors (Agarwal *et al.,* 2014; Christensen *et al.,* 2011). Overall, these data suggest that directly targeting c-Myc for degradation or regulating the molecular control of its stability has potential therapeutic value for cancer treatment (Janghorban *et al.,* 2014).

Consistent with the above, our experiments exhibited that EMD could induce c-Myc degradation in lung cancer cells. EMD was demonstrated to possess a potent effect on c-Myc-targeted degradation. Our results indicated that while the other protein markers that we evaluated in this study were not affected by EMD treatment, the level of the c-Myc protein was strongly depleted (Figures 3C–D).

In this study, we found that after EMD treatment, the half-life of the c-Myc protein was shortened. The cycloheximide chasing assay showed that the half-life of c-Myc in response to 100 μM was approximately 12 and 15 minutes compared to 23 and 20 minutes in non-treated H292 and H23 cells, respectively (Figures 4A–C). After MG132, as a selective proteasome inhibitor, was applied, the c-Myc protein level in EMD-treated cells was significantly restored, demonstrating that proteasomal degradation plays a role in c-Myc function. Consistent with our results (Figures 4D–E and 5L–M), inhibition of the proteasome function by the proteasome inhibitor lactacystin could restore the level of c-Myc *in vivo* (Gregory and Hann, 2000). Furthermore, we evaluated the levels of the c-Myc–ubiquitin complex and found that the formation of the complex was remarkably elevated in the EMD-treated cells. In the last section, we reported how EMD demonstrated potential anticancer activity not only in universal lung cancer cell lines, but also primary lung cancer cells and leukemia cells. We found that all the other cell types used in this study showed strongly induced apoptotic cell death in a dose dependent-manner. The c-Myc protein levels were dramatically depleted after treatment with 100 μM EMD. At this point, these results strongly support the conclusion that EMD could be a candidate anticancer compound by targeting c-Myc degradation through the ubiquitin–proteasomal pathway in several types of cancer cells. Moreover, etoposide was used for comparison with EMD and found that when used at the same concentrations EMD showed greater cytotoxic effect (Figure 5E). Because etoposide resistance can be frequently found in

an aggressive lung cancer (Shanker *et al.*, 2010; Hopper-Borge et al, 2013; Kim, 2016; Wang 2019), EMD may benefit the treatment of etoposide resistant cancer.

Finally, the effect of EMD against the c-Myc protein in normal cells was evaluated. The results in HaCAT and HK2 cells differed from each other and showed that the effect of EMD may be cell-type specific. c-Myc is a part of several essential mechanisms in normal cells and is strictly regulated by ubiquitin-proteasomal degradation and other interacting proteins (Stine *et al.,* 2015). However, there are alterations of c-Myc regulation were reported in cancerous cells. Indeed, mutation and inactivation of some MYC E3 ligases were reported. Fbw7 functioning as c-Myc ligase was shown to be inactivated in cancers (O'Neil *et al.*, 2007; Tan *et al.*, 2008) and the deletion of its gene *FBW7* was found in approximately 30% of human cancers (Knuutila *et al.*, 1999; Welcker *et al.,* 2004; Yeh *et al.,* 2018). In addition, Usp28, an antagonist of c-Myc ligase Fbw7α, was shown to be overexpressed in cancer (Popov *et al.*, 2007b; Shi *et al.,* 2010). Also, TRUSS, c-Myc E3 ligase, was reported to be down-regulated in many cancer cells (Choi *et al.,* 2010). The different responses to EDM-mediated c-Myc down-regulation found in this study is likely caused by the alteration of c-Myc control mechanisms or different up-stream signals that specific to cell type and condition. Results of EMD in targeting c-Myc in cancerous and normal cells may at least provide additional information of this compound and encourage the investigations of the c-Myc regulatory mechanism that specific for cancer cells.

In conclusion, this study provides contributing evidence for EMD to be considered a candidate anticancer therapy for several cancer types. EMD was shown to have a tremendous apoptotic induction capability with various cell types. Also, the mechanism of action of EMD is quite specific. The compound plays a role in c-Myc depletion by enhancing ubiquitin–proteasomal degradation of the c-Myc protein. As c-Myc was exhibited to be an essential factor

Molecular Pharmacology Fast Forward. Published on June 2, 2020 as DOI: 10.1124/mol.120.119719
This article has not been copyedited and formatted. The final version may differ from this version.

for cancer cell proliferation and survival, these data might be advantageous for emphasizing EMD as a candidate compound in anticancer research (Figure 6).

Molecular Pharmacology Fast Forward. Published on June 2, 2020 as DOI: 10.1124/mol.120.119719
This article has not been copyedited and formatted. The final version may differ from this version.

Acknowledgements

We sincerely thank Cell-based drug and health product development research unit, Faculty of Pharmaceutical Science, Chulalongkorn university and Siriraj Center of Excellence for Stem Cell Research, Siriraj hospital, Mahidol University, Thailand. In addition, the Scholarship from the Graduate School, Chulalongkorn University to commemorate the 72nd anniversary of his Majesty King Bhumibol Adulyadej is gratefully acknowledged.

Molecular Pharmacology Fast Forward. Published on June 2, 2020 as DOI: 10.1124/mol.120.119719
This article has not been copyedited and formatted. The final version may differ from this version.

Authorship contributions

Participated in research design: Chanvorachote, Luanpitpong

Conducted experiments: Sriratanasak, Petsri, Wattanathana

Contributed new reagents or analytic tools: Laobuthee, Vinayanuwattikun

Performed data analysis: Sriratanasak, Chanvorachote, Luanpitpong

Wrote or contributed to the writing of the manuscript: Sriratanasak, Wattanathana, Luanpitpong, Chanvorachote

Molecular Pharmacology Fast Forward. Published on June 2, 2020 as DOI: 10.1124/mol.120.119719
This article has not been copyedited and formatted. The final version may differ from this version.

References

Agarwal A, MacKenzie RJ, Pippa R, Eide CA, Oddo J, Tyner JW, Sears R, et al. (2014) Antagonism of SET using OP449 enhances the efficacy of tyrosine kinase inhibitors and overcomes drug resistance in myeloid leukemia. *Clin Cancer Res* **20**:2092–2103.

Amati B, and Sanchez-Arévalo Lobo VJ (2007) MYC degradation: Deubiquitinating enzymes enter the dance. *Nat Cell Biol* **9**: 729-731.

Allen- Petersen B and Sears R (2019) Mission Possible Advances in MYC Therapeutic Targeting in Cancer. *BioDrugs* **33**(5):539-553.

Baig S, Seevasant I, Mohamad J, Mukheem A, Huri HZ, and Kamarul T (2016) Potential of apoptotic pathway-targeted cancer therapeutic research: Where do we stand. *Cell Death Dis* **7**: e2058.

Bock FJ, and Tait SWG (2019) Mitochondria as multifaceted regulators of cell death. *Nat Rev Mol Cell Biol*.

Brägelmann J, Böhm S, Guthrie MR, Mollaoglu G, Oliver TG, and Sos ML (2017) Family matters: How MYC family oncogenes impact small cell lung cancer. *Cell Cycle* **16**:1489–1498.

Bressin C, Bourgarel-Rey V, Carré M, Pourroy B, Arango D, Braguer D, and Barra Y (2006) Decrease in c-Myc activity enhances cancer cell sensitivity to vinblastine. *Anticancer Drugs* **17**:181-187.

Carabet LA, Rennie PS, and Cherkasov A (2019) Therapeutic inhibition of myc in cancer. Structural bases and computer-aided drug discovery approaches. *Int J Mol Sci* **20**.

Cha G, Xu J, Xu X, Li B, Lu S, Nanding A, et al. (2017) High expression of CIP2A protein is associated with tumor aggressiveness in stage I-III NSCLC and correlates with poor

prognosis. *Onco Targets Ther* **10**:5907–5914.

Chen H, Liu H, and Qing G (2018) Targeting oncogenic Myc as a strategy for cancer treatment. *Signal Transduct Target Ther* **3.**

Chirachanchai S, Laobuthee A, and Phongtamrug S (2009) Self termination of ring opening reaction of p-substituted phenol-based benzoxazines: An obstructive effect via intramolecular hydrogen bond. *J Heterocycl Chem* **46**: 714-721.

Choi SH, Wright JB, Gerber SA and Cole MD (2010) Myc protein is stabilized by suppression of a novel E3 ligase complex in cancer cells. Genes Dev **24**:1236–1241.

Christensen DJ, Chen Y, Oddo J, Matta KM, Neil J, Davis ED, et al. (2011) SET oncoprotein overexpression in B-cell chronic lymphocytic leukemia and non-Hodgkin lymphoma: A predictor of aggressive disease and a new treatment target. *Blood* **118**:4150–4158.

Come C, Laine A, Chanrion M, Edgren H, Mattila E, Liu X, et al. (2009) CIP2A is associated with human breast cancer aggressivity. *Clin Cancer Res* **15**:5092–5100.

Comis RL, Friedland DM and Good BC (1999) The Role of Oral Etoposide in Non-Small Cell Lung Cancer. *Drugs* **58** (Suppl 3):21-30.

Conacci-Sorrell M, McFerrin L, and Eisenman RN (2014) An overview of MYC and its interactome. *Cold Spring Harb Perspect Med* **4**.

Cosaert J and Quoix E (2002) Platinum drugs in the treatment of non-small-cell lung cancer. *Br J Cancer* **87**:825–833.

Daniel H (2012) MYC on the path to cancer. *Cell* **76**:211-220.

Dragoj M, Bankovic J, Podolski-Renic A, Buric SS, Pesic M, Tanic N, and Stankovic T (2019) Association of overexpressed MYC gene with altered PHACTR3 and E2F4 genes contributes to non-small cell lung carcinoma pathogenesis. *J Med Biochem* **38**:188–195.

Elbadawy M, Usui T, Yamawaki H, and Sasaki K (2019) Emerging roles of C-myc in cancer stem cell-related signaling and resistance to cancer chemotherapy: A potential therapeutic target against colorectal cancer. *Int J Mol Sci* **20**.

Farrell AS and Sears RC (2014) MYC Degradation. *Cold Spring Harb Perspect Med* **4**:a014365.

Felsher DW, and Bishop JM (1999) Reversible tumorigenesis by MYC in hematopoietic lineages. *Mol Cell* **4**:1024-1039.

Furuse K (1992) Platinum/Oral Etoposide Therapy in Non-Small Cell Lung Cancer. *Oncol* **49** (Suppl 1):63-69.

Gabay M, Li Y and Felsher DW (2014) MYC Activation Is a Hallmark of Cancer Initiation and Maintenance. *Cold Spring Harb Perspect Med* **4**: a014241.

Goebel C, Louden C, Mckenna R, Onugha O, Wachtel A and Long T (2019) Diagnosis of Non-small Cell Lung Cancer Cancer for Early Stage Asymptomatic Patients. *Cancer Genom Proteom* **16**(4): 229-244.

Gregory MA, and Hann SR (2000) c-Myc Proteolysis by the Ubiquitin-Proteasome Pathway: Stabilization of c-Myc in Burkitt's Lymphoma Cells. *Mol Cell Biol* **20**:2423-35.

Hopper-Borge (2013) Drug Resistance Mechanisms in Non-Small Cell Lung Carcinoma. *J Cancer Res* **2**:265-282.

Huang HL, Weng HY, Wang LQ, Yu CH, Huang QJ, Zhao PP, et al. (2012) Triggering Fbw7-mediated proteasomal degradation of c-Myc by oridonin induces cell growth inhibition and apoptosis. *Mol Cancer Ther* **11**:1155–1165.

Huang H, Weng H, Zhou H, and Qu L (2014) Attacking c-Myc: Targeted and Combined Therapies for Cancer. *Curr Pharm Des* **20**:6543-6554.Igney F and Krammer P (2002) Death

and Anti-death Tumour. *Nat Rev Cancer* **2**(4): 277-288.

Janghorban M, Farrell AS, Allen-Petersen BL, Pelz C, Daniel CJ, Oddo J, et al. (2014) Targeting c-MYC by antagonizing PP2A inhibitors in breast cancer. *PNAS* **111**:9157-9162.

Kaewvilai A, Rujitanapanich S, Wattanathana W, Veranitisagul C, Suramitr S, Koonsaeng N, and Laobuthee A (2012) The effect of alkali and ce(III) ions on the response properties of benzoxazine supramolecules prepared via molecular assembly. *Int J Mol Sci* **17**:1074.

Kalkat M, De Melo J, Hickman KA, Lourenco C, Redel C, Resetca D, Tamachi A, Tu WB, and Penn LZ (2017) MYC deregulation in primary human cancers. *Genes (Basel)* **8**:2-30.

Kao SH, Wang WL, Chen CY, Chang YL, Wu YY, Wang YT, Wang SP, Nesvizhskii A, Chen YJ, Hong TM, and Yang PC (2015) Analysis of Protein Stability by the Cycloheximide Chase Assay. *Bio-Protocol* **5**.

Kim ES (2016) Chemotherapy Resistance in Lung Cancer. *Adv Exp Med Biol* **893**:189-209.

Knapp DC, Mata JE, Reddy MT, Devi GR, and Iversen PL (2003) Resistance to chemotherapeutic drugs overcome by c-Myc inhibition in a Lewis lung carcinoma murine model. *Anticancer Drugs* **14**:39-47.

Knuutila S, Aalto Y, Autio K, Bjorkqvist AM, El-Rifai W, Hemmer S, Huhta T, Kettunen E, Kiuru-Kuhlefelt S, Larramendy ML, et al. (1999) DNA copy number losses in human neoplasms. Am J Pathol **155**:683–694.

Kumar N, Yadav N, Amarnath N, Sharma V, Shukla S, Srivastava A, Prasad P, Kumar A, Garg S, Singh S, Sehrawat S, and Lochab B (2019) Integrative natural medicine inspired graphene nanovehicle-benzoxazine derivatives as potent therapy for cancer. *Mol Cell Biochem* **454**:123-138.

Li YQ, Pu J, Guan H, Ji M, Shi B, Chen M, et al. (2018) c-Myc Is a Major Determinant for

Antitumor Activity of Aurora A Kinase Inhibitor MLN8237 in Thyroid Cancer. *Thyroid* **28**:1642-1654.

O'Neil J, Grim J, Strack P, Rao S, Tibbitts D, Winter C, Hardwick J, Welcker M, Meijerink JP, Pieters R, et al. (2007) FBW7 mutations in leukemic cells mediate NOTCH pathway activation and resistance to γ-secretase inhibitors. J Exp Med **204**:1813–1824.

Pan XN, Chen JJ, Wang LX, Xiao RZ, Liu LL, Fang ZG, Liu Q, Long ZJ, and Lin DJ (2014) Inhibition of c-Myc overcomes cytotoxic drug resistance in acute myeloid leukemia cells by promoting differentiation. *PLoS One* **9**.

Pelengaris S, Khan M, and Evan G (2002) c-MYC: More than just a matter of life and death. *Nat Rev Cancer* **2**:764-776.

Pollard TD, Earnshaw WC, Lippincott-Schwartz J and Johnson GT, editors (2017) Chapter 46 - Programmed Cell Death. *Cell Biology*. **3rd ed**. Philadelphia, PA: Elsevier:797-813.

Popov N, Wanzel M, Madiredjo M, Zhang D, Beijersbergen R, Bernards R, Moll R, Elledge SJ, Eilers M (2007) *Nat Cell Biol* **9**:65-74.

Reck M, Popat S, Reinmuth N, De Ruysscher D, Kerr K and Peters S (2014) Metastatic non-small- cell lung cancer (NSCLC) : ESMO Clinical Practice Guidelines for diagnosis, treatment and follow-up. *Ann Oncol* **25**(suppl 3):iii27-iii39.

Ruckdeschel JC (1991) Etoposide in the Management of Non-Small Cell Lung Cancer. *Cancer* **67** (Suppl 1):250-253.

Sallam M, Wong H and Escriu C (2019) Treatment beyond four cycles of first line Platinum and Etoposide chemotherapy in real-life patients with stage IV Small Cell Lung Cancer: a retrospective study of the Merseyside and Cheshire Cancer network. *BMC Pulm Med* **19**: 195.

Sears R, Nuckolls F, Haura E, Taya Y, Tami K and Nevins JR (2000) Multiple Ras-dependent phosphorylation pathways regulate Myc protein stability. *Genes Dev* **14**:2501–2514.

Sears RC (2004) The life cycle of c-Myc: From synthesis to degradation. *Cell Cycle* **3**:1133-1137.

Shanker M, Willcutts D, Roth JA, and Ramesh R (2010) Drug resistance in lung cancer. *Lung Cancer: Targets and Therapy* **1**:23-36.

Shi D and Grossman SR (2010) Ubiquitin becomes ubiquitous in cancer: emerging roles of ubiquitin ligases and deubiquitinases in tumorigenesis and as therapeutic targets. *Cancer Biol Ther* **10**:737-747.

Siegel R, Miller K, and Jemal A (2016) cancer statistic, 2016. *CA Cancer J Clin* **66**(1):7-30.

Siegel RL, Miller KD, and Jemal A (2019) Cancer statistics, 2019. *CA Cancer J Clin* **69**:7-34.

Stine Z, Walton Z, Altman B, Hsieh A and Dang C (2015) myc metabolism and cancer. *Cancer Discov* **5**(10):1024-1039.

Tan Y, Sangfelt O and Spruck C (2008) The Fbxw7/hCdc4 tumor suppressor in human cancer. Cancer Lett **271**:1–12.

Vansteenkiste J, De Ruysscher D, Eberhardt WEE, Lim E, Senan S, Felip E, and Peters S (2013) Early and locally advanced non-small-cell lung cancer (NSCLC): ESMO clinical practice guidelines for diagnosis, treatment and follow-up.

Veranitisagul C, Kaewvilai A, Sangngern S, Wattanathana W, Suramitr S, Koonsaeng N, and Laobuthee A (2011) Novel recovery of nano-structured ceria (CeO 2) from Ce(III)-benzoxazine dimer complexes via thermal decomposition. *Ann Oncol* **24**.

Vinayanuwattikun C, Prakhongcheep O, Tungsukruthai S, Petsri K, Thirasastr P, Leelayuwatanakul N and et al (2019) Feasibility Technique of Low‐passage In Vitro Drug

Sensitivity Testing of Malignant Pleural Effusion from Advanced-stage Non-small Cell Lung Cancer for Prediction of Clinical Outcome. *Anticancer Res* **39**(12):6981-6988.

Vita M, and Henriksson M (2006) The Myc oncoprotein as a therapeutic target for human cancer. *Semin Cancer Biol* **16**:318-330.

Wang X, Zhang H and Chen X (2019) Drug Resistance and Combating Drug Resistance in Cancer. *Cancer Drug Resist* **2**:141-160.

Wattanathana W, Nonthaglin S, Veranitisagul C, Koonsaeng N and Laobuthee A. (2014) Crystal structure and novel solid-state fluorescence behaviorof the model benzoxazine monomer 3,4-Dihydro-3,6-dimethyl-1,3,2H-benzoxazine. *J Mol Struct* **1074**: 118-125.

Wattanathana W, Nootsuwan N, Veranitisagul C, Koonsaeng N, Suramitr S and Laobuthee A (2016) Crystallographic, spectroscopic (FT-IRFT-Raman) and computational (DFTB3LYP) studies on 4,4′-diethyl-2,2′-[methylazanediylbis(methylene)]diphenol. *J Mol Struct* **1109**: 201-208.

Welcker M, Orian A, Grim JA, Eisenman RN and Clurman BE (2004) A Nucleolar Isoform of the Fbw7 Ubiquitin Ligase Regulates c-Myc and Cell Size. *Curr Biol* **14**: 1852-1857.

Westermarck J, Hahn WC (2008) Multiple pathways regulated by the tumor suppressor PP2A in transformation. *Trends Mol Med* **14**:152–160.

Whitfield JR, Beaulieu ME, and Soucek L (2017) Strategies to inhibit Myc and their clinical applicability. *Front Cell Dev Biol* **5**.

Xia B, Tian C, Guo S, Zhang L, Zhao D, Qu F, Zhao W, Wang Y, Wu X, Da W, Wei S, and Zhang Y (2015) C-Myc plays part in drug resistance mediated by bone marrow stromal cells in acute myeloid leukemia. *Leuk Res* **39**:92-99.

Yeh CH, Bellon M and Nicot C (2018) FBXW7: a critical tumor suppressor of human cancers. *Mol Cancer* **17**:115.

Zahavi D and Weiner L. (2019) Tumor mechanisms of resistance to immune attack. Prog Mol Biol Transl. **164**:61-100.

Zappa C, and Mousa SA (2016) Non-small cell lung cancer: Current treatment and future advances. *Transl Lung Cancer Res* **5**:288-300.

Zhang J, Zhou L, Nan Z, Yuan Q, Wen J, Xu M, Li Y, Li B, Wang P, Liu C, Ma Y, Chen S, and Xie S (2017) Knockdown of c-Myc activates Fas-mediated apoptosis and sensitizes A549 cells to radiation. *Oncol Rep* **38**:2471-2479.

Footnotes

a) This work was supported by the Thailand Research Fund [Grant RSA6180036].

b) –

c) Pithi Chanvorachote, Ph. D. , Department of Pharmacology and Physiology, Faculty of Pharmaceutical Sciences, and Cell- based Drug and Health Product Development Research Unit, Phayathai Road, Pathumwan, Chulalongkorn University, Bangkok, Thailand 10330
Email: pithi.ch@gmail.com

d) –

Molecular Pharmacology Fast Forward. Published on June 2, 2020 as DOI: 10.1124/mol.120.119719
This article has not been copyedited and formatted. The final version may differ from this version.

Legends for the figures

Figure 1. Synthesis and characterization of EMD. (A) Synthesis of EMD comprising two steps: a Mannich reaction (step 1) and ring-opening dimerization (step 2). (B) FTIR spectrum of the EMD compound. (C) Ortep plot showing a 50% probability level of the compound EMD at 100 K.

Figure 2. EMD inhibits cell proliferation and induces apoptosis in NSCLC H292 and H23 cells. (A) MTT assay was used to evaluate cell viability after treatment with various concentrations of EMD (0–100 μM) for 24 hours. (B) The half-maximal inhibitory concentrations (IC_{50}) of EMD against H292 and H23 cells were calculated from MTT assay by comparison with an untreated control. (C–D) H292 and H23 cells were treated with EMD (0–100 μM) for 24 hours and then stained with Hoechst 33342. The images were visualized using an inverted fluorescence microscope. The condensed blue fluorescence of Hoechst 33342 represents the fragmented chromatin in apoptotic cells. (E–F) H292 and H23 cells were treated with EMD (0–100 μM) for 24 hours and the percentage of dead cells in each stage was evaluated by annexin V-FITC/PI staining with flow cytometry. The percentages of cells in each stage are presented as the mean ± SD and the percentage of apoptotic cells between each concentration of EMD compared with the non-treatment control were statistical calculated by repeated measured one-way ANOVA with Schefft's post-hoc test. (n = 3) (* $0.01 \leq p < 0.05$, ** $p < 0.01$). (G–H) H292 and H23 cells were treated with EMD (0–100 μM) for 24 hours and then stained with Hoechst 33342. Cell cycle analysis was evaluated by flow cytometry and the percentages of the cell cycle distribution in each phase are presented.

Figure 3. EMD triggers the apoptotic markers and downregulates c-Myc in lung carcinoma. NSCLC H292 and H23 cells were treated with EMD (0–100 μM) for 24 hours. (A, C) Western blot analysis was performed to measure the apoptotic-related proteins. β-actin

protein was evaluated to confirm the equal loading of each protein sample. (B, D) Densitometry of each protein levels was calculated and the results are presented as a relative protein level. The statistical calculation was compiled with repeated measured one-way ANOVA with Schefft's post-hoc test. Data represent the mean ± SD (n = 3) (* $0.01 \leq p < 0.05$, ** $p < 0.01$, compared with the untreated control).

Figure 4. EMD induces ubiquitin-mediated c-Myc proteasomal degradation. (A) The half-life of c-Myc was confirmed using the cycloheximide (CHX) chasing assay. H292 and H23 cell lines were treated with 50 μg/ml of CHX with or without 100 μM EMD as indicated by the time in minutes. Western blot analysis was performed to evaluate the c-Myc protein levels. (B) The relative c-Myc protein levels were calculated and compared with the non-treatment control at 0 minute. (C) The half-lives of the c-Myc protein of H292 and H23 cells were calculated. (D–E) H292 and H23 cell lines were pre-treated with MG 132 (0–20 μM) as a potent proteasome inhibitor for 1 hour and then treated with EMD (0–100 μM) for 1 hour. c-Myc protein levels were measured by western blot analysis. (F–G) H292 and H23 cells were pre-treated with MG132 10 μM for 30 minutes followed by treatment with EMD 100 μM for 1 hour. The protein lysates were collected and incubated with a mixture of beads and c-Myc primary antibodies to pull out the protein of interest. Then, the ubiquitinated protein levels were measured by western blot analysis. The statistical calculation was compiled with repeated measured one-way ANOVA with Schefft's post-hoc test for individual comparisons and t-test for two group comparison. The relative to control protein levels are reported. (n = 3) (* $0.01 \leq p < 0.05$, ** $p < 0.01$)

Figure 5. EMD demonstrated the potential to inhibit cell proliferation and promote apoptosis cell death in K562 and all four primary cell lines. (A–B) Hoechst staining assay was performed in K562 cells after treatment with various concentrations of EMD for 24 hours and the percentage of apoptotic cell death was calculated. (C–D) c-Myc protein levels were

evaluated by western blot analysis and the relative protein levels were calculated. (E) MTT assay was performed to evaluate cell viability after treatment with EMD and etoposide at the same concentrations (0–100 μM) for 24 hours. (F–G) Cell viabilities of the four primary cell lines were strongly decreased and the half-maximal inhibitory concentrations (IC_{50}) of EMD against four cell lines were calculated. (H–I) Four primary cell lines were treated with EMD and etoposide (0–100 μM) for 24 hours before staining with Hoechst 33342 and the images captured under an inverted fluorescence microscope. (J–K) Western blot was performed to analyze the c-Myc protein levels. Densitometry of the c-Myc protein levels was calculated and the results presented as relative protein levels. (L–M) K562 and four primary cell lines were pre-treated with MG 132 (0–10 μM) potent proteasome inhibitor for 1 hour and treated with EMD (100 μM) for 1 hour. c-Myc protein levels were measured by western blot analysis. (N–O) HaCAT and HK2 cells were treated with EMD (0–100 μM) for 24 hours. Western blot analysis was performed to measure the c-Myc protein level. β-actin protein was evaluated to confirm an equal loading of each protein sample. Densitometry of each protein level was calculated and presented as a relative protein level. The statistical calculation was compiled with repeated measured one-way ANOVA with Schefft's post-hoc test. Data represent the mean ± SD (n = 3) (* $0.01 \leq p < 0.05$, ** $p < 0.01$).

Figure 6. Deregulation of c-Myc. The oncoprotein takes part in several survival mechanisms of cancer cells that support the disease progression and treatment failure, such as genomic instability, uncontrolled cell proliferation, and deficiency of immune surveillance, independent of growth factors. EMD enhances the apoptotic cell death of cancer cells and specifically triggers the ubiquitin–proteasome degradation of c-Myc.

Table 1 Characteristics of the primary cell lines derived from patients, showing the types of lung cancer, molecular alteration, and characteristics of each patient.

Table 1

Cell lines	Tissue	Pathology	Molecular alteration	Patient character		
				Sex	Age (year)	Treatment
ELC12	pleural effusion	Lung squamous cell carcinoma	N/A	Female	71	Naïve
ELC16	pleural effusion	Lung adenocarinoma	EGFR exon 19 del, ALK WT	Female	33	CK 101, tyrosine kinase inhibitor
ELC17	pleural effusion	Lung adenocarinoma	N/A	Female	77	carboplatin/pactalixel/avastin
ELC20	pleural effusion	Lung adenocarinoma	EGFR exon 19 del	Female	51	Naïve

Molecular Pharmacology Fast Forward. Published on June 2, 2020 as DOI: 10.1124/mol.120.119719
This article has not been copyedited and formatted. The final version may differ from this version.

Figure 1

A

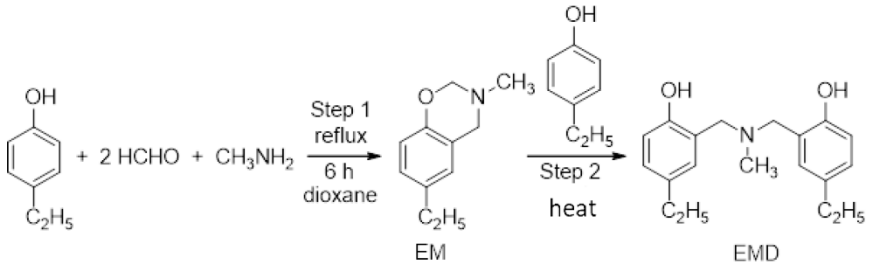

B

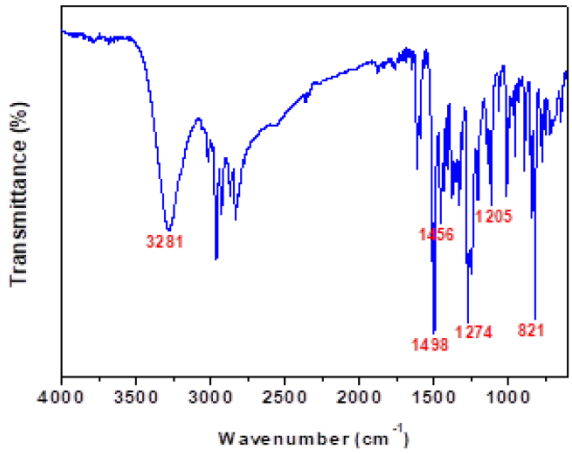

C

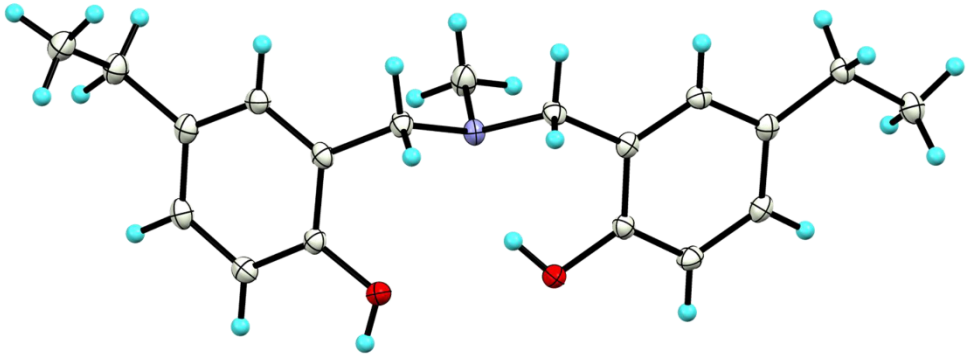

Molecular Pharmacology Fast Forward. Published on June 2, 2020 as DOI: 10.1124/mol.120.119719
This article has not been copyedited and formatted. The final version may differ from this version.

Figure 2

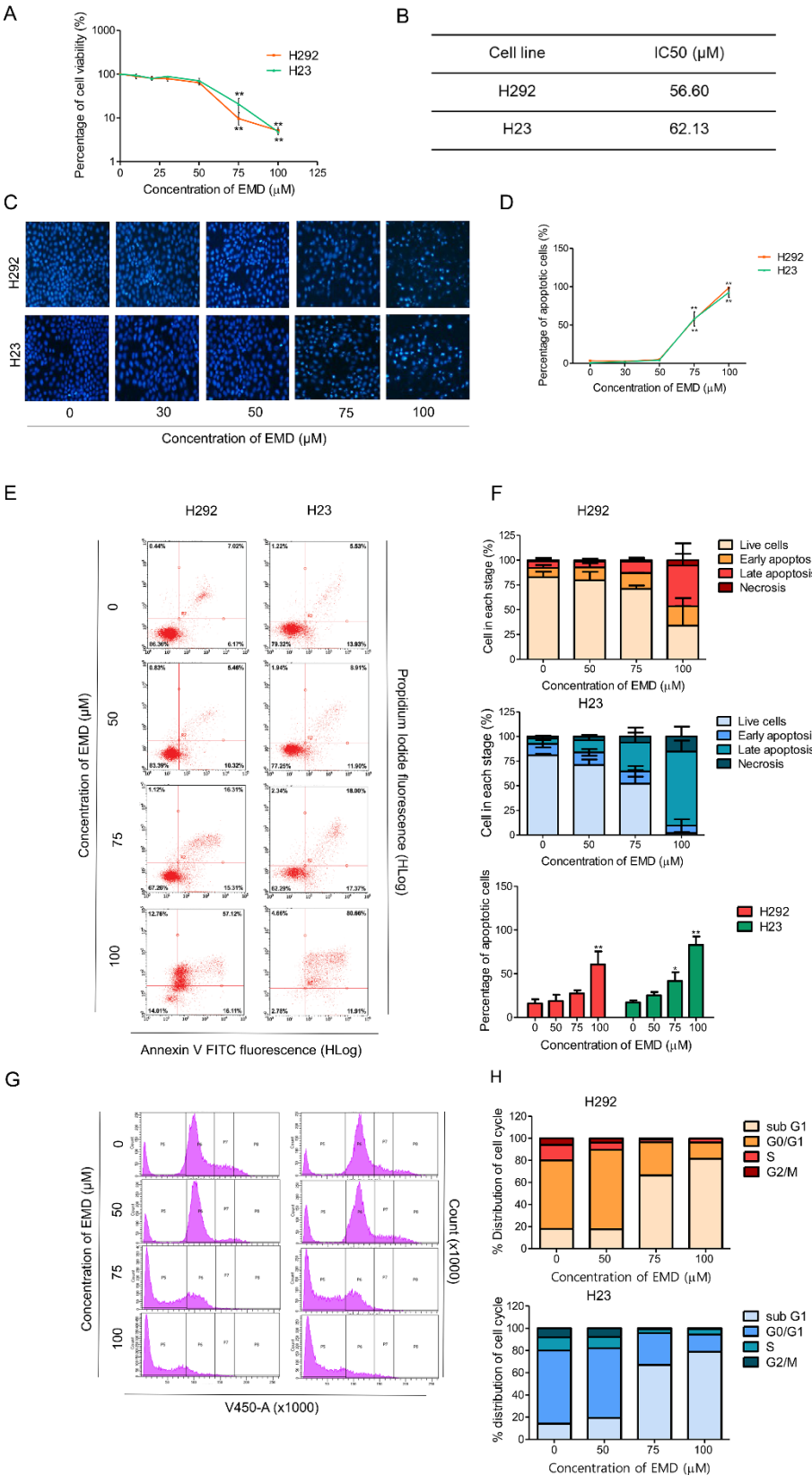

Molecular Pharmacology Fast Forward. Published on June 2, 2020 as DOI: 10.1124/mol.120.119719
This article has not been copyedited and formatted. The final version may differ from this version.

Figure 3

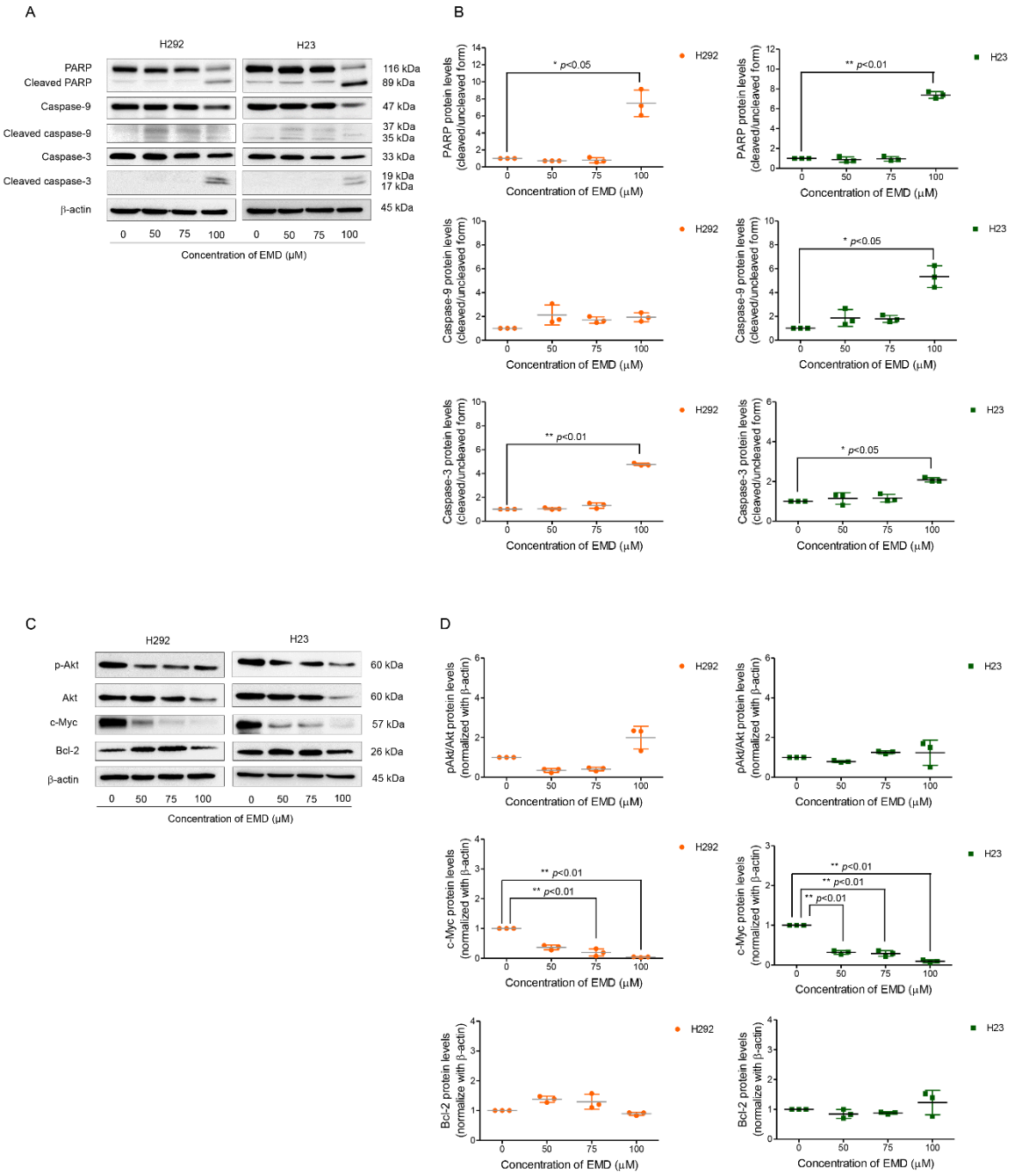

Molecular Pharmacology Fast Forward. Published on June 2, 2020 as DOI: 10.1124/mol.120.119719
This article has not been copyedited and formatted. The final version may differ from this version.

Figure 4

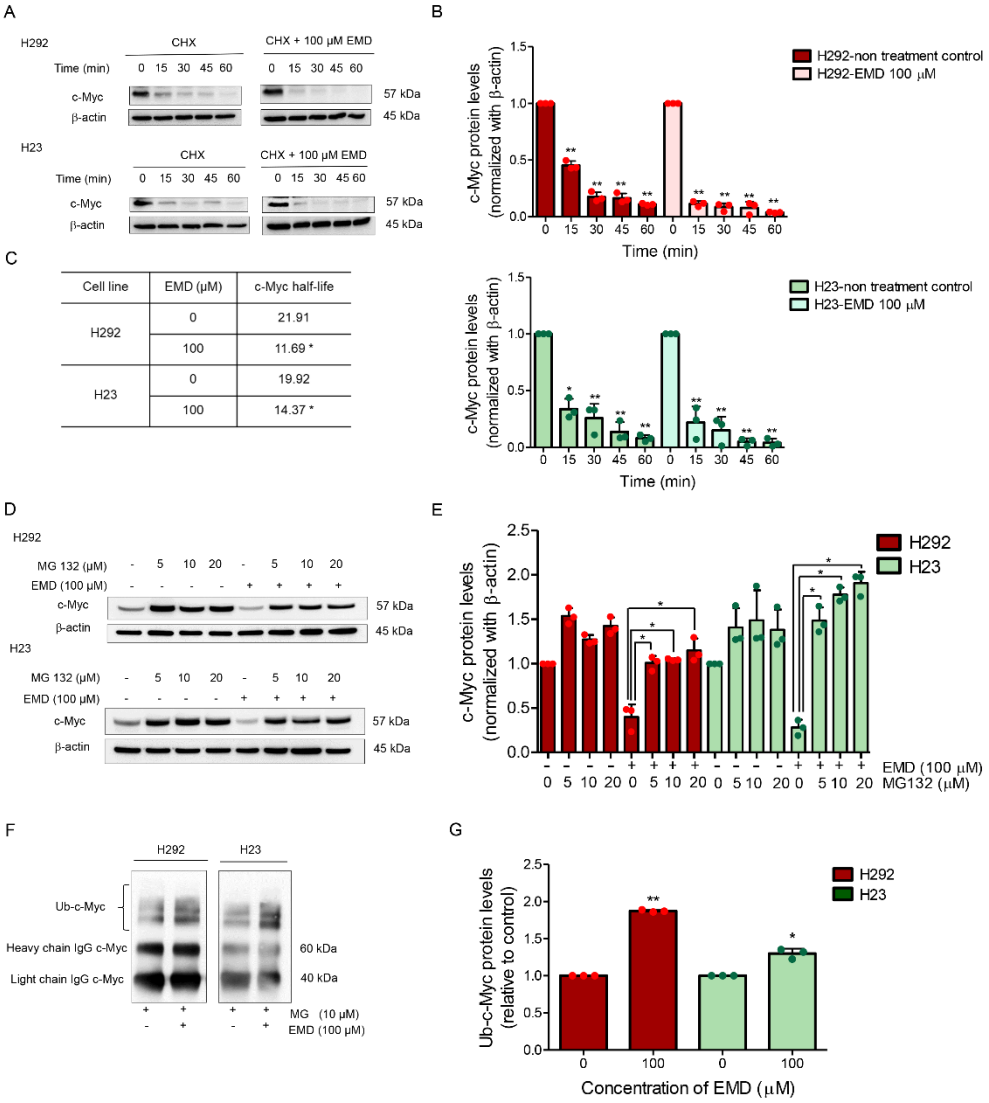

Molecular Pharmacology Fast Forward. Published on June 2, 2020 as DOI: 10.1124/mol.120.119719
This article has not been copyedited and formatted. The final version may differ from this version.

Figure 5

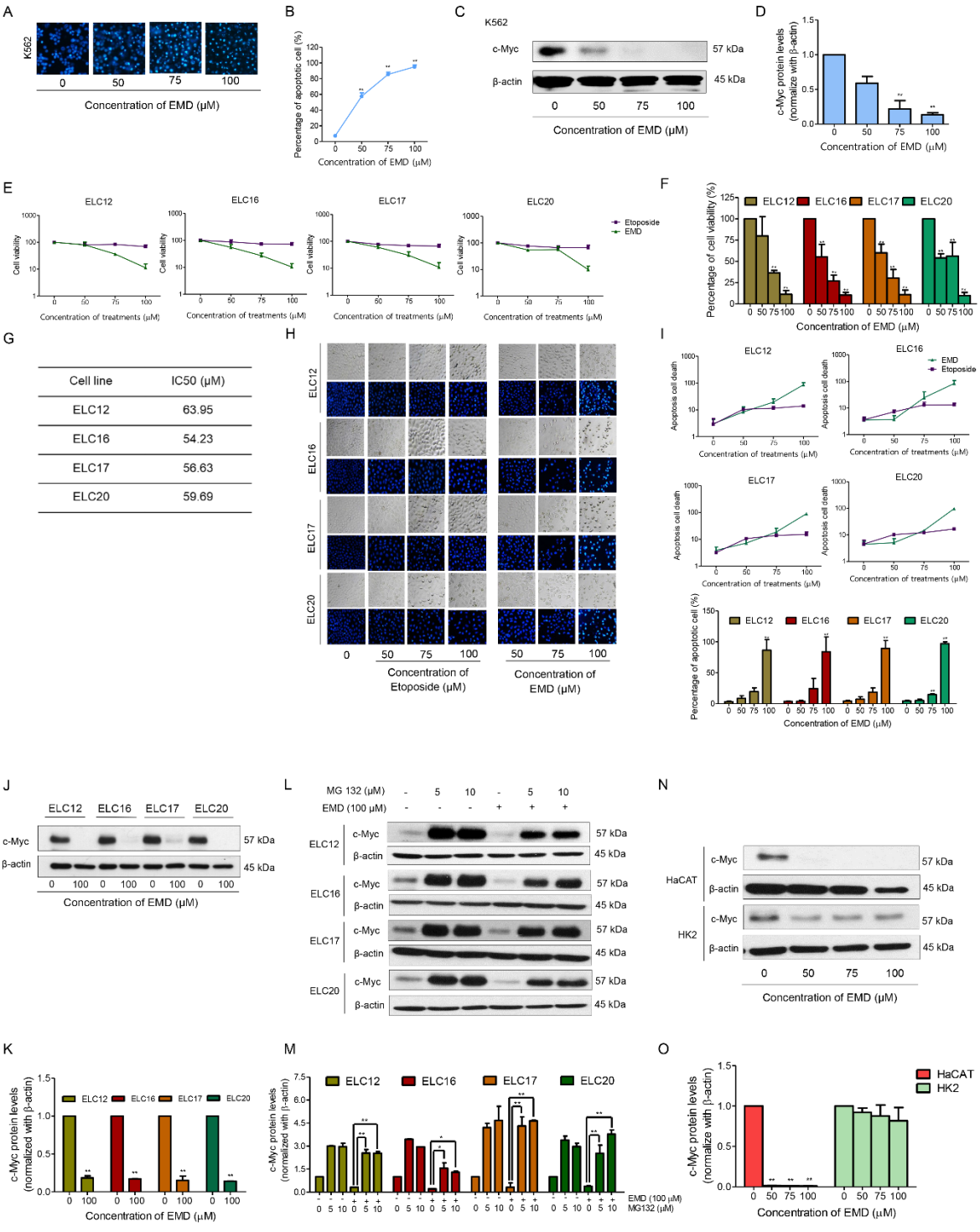

Molecular Pharmacology Fast Forward. Published on June 2, 2020 as DOI: 10.1124/mol.120.119719
This article has not been copyedited and formatted. The final version may differ from this version.

Figure 6